Journal of Solid State Chemistry 264 (2018) 119–123

Contents lists available at ScienceDirect

Journal of Solid State Chemistry

journal homepage: www.elsevier.com/locate/jssc

Magnetic ordering in the layered oxyselenides $Sr_2CoO_2Ag_2Se_2$ and $Ba_2CoO_2Ag_2Se_2$

Sebastian J.C. Herkelrath[a], Jack N. Blandy[a,b], Simon J. Clarke[a,*]

[a] Department of Chemistry, University of Oxford, Inorganic Chemistry Laboratory, South Parks Road, Oxford OX1 3QR, United Kingdom
[b] Diamond Light Source Ltd., Harwell Science and Innovation Campus, Didcot OX11 0DE, United Kingdom

ARTICLE INFO

Keywords:
Oxychalcogenide
Oxide selenide
Antiferromagnetic order

ABSTRACT

The antiferromagnetic structures of $Sr_2CoO_2Ag_2Se_2$ and $Ba_2CoO_2Ag_2Se_2$ are solved using powder neutron diffraction. Both compounds adopt the same magnetic structure, based on a $\sqrt{2}a \times \sqrt{2}a \times c$ expansion of the nuclear cell with magnetic space group P_C4_2/n (86.72 in the Belov-Neronova-Smirnova notation). This structure is adopted as a result of nearest-neighbour antiferromagnetic interactions within the CoO_2 planes. The refined long-range-ordered magnetic moments of $Sr_2CoO_2Ag_2Se_2$ and $Ba_2CoO_2Ag_2Se_2$ are 3.7(1) and 3.97(3) μ_B per Co ion respectively. The refined moments are significantly greater than the value predicted from just considering the spin (3 μ_B); this is attributed to a significant orbital contribution to the magnetic moment in an analogous manner to that previously observed for $Sr_2CoO_2Cu_2S_2$ and the values conform to a relationship between the shape of the distended CoO_4Ch_2 (*Ch* = S, Se) octahedron and the size of the ordered moment established for a series of related compounds.

1. Introduction

The synthesis and characterisation of the first layered cobalt oxychalcogenides, $A_2CoO_2Cu_2S_2$ (*A* = Sr, Ba), were reported by Zhu et al. [1] These compounds adopted the $Sr_2Mn_3Sb_2O_2$ structure type [2], with alternating square planar CoO_2 and antifluorite-type Cu_2S_2 layers with A^{2+} cations situated in between, as shown in Fig. 1. This structure is adopted by compounds with a wide range of anions and cations as described elsewhere [3].

These solids have attracted significant interest because they represent an unusual example of high spin Co^{2+} in a coordination environment that describes a greatly distended CoO_4Ch_2 (*Ch* = S, Se) octahedron which can be considered as tending to square planar (i.e. approaching square planar CoO_4). A small copper deficiency in $Sr_2CoO_2Cu_{2-x}S_2$ was reported by Zhu et al. [1], and subsequent work by Smura et al. revealed that $Sr_2CoO_2Cu_2S_2$ could be synthesised stoichiometrically, but a Cu deficiency of up to about 5% was induced by reaction of $Sr_2CoO_2Cu_2S_2$ with moist air [4]. The same report by Smura et al. showed that the magnetic structure of both $Sr_2CoO_2Cu_2S_2$ and $Ba_2CoO_2Cu_2S_2$ was based on the antiferromagnetic coupling of nearest-neighbour Co^{2+} ions within the CoO_2 planes [4]. The refined moment on each Co^{2+} ion was 3.81(6) μ_B for stoichiometric $Sr_2CoO_2Cu_2S_2$ and 4.45(9) μ_B for $Ba_2CoO_2Cu_2S_2$. These values are both much larger than the 3 μ_B maximum expected for ordered high spin Co^{2+} moments using the spin-only approximation. With the assistance of computation, this discrepancy was attributed to a large unquenched orbital contribution to the magnetic moment which increased as the Co^{2+} coordination environment became increasingly square planar [4]. The ordered magnetic moment of a sample of $Sr_2CoO_2Cu_{2-x}S_2$ that had been exposed to moist O_2 was 2.44(6) μ_B, far below the value obtained for stoichiometric $Sr_2CoO_2Cu_2S_2$. This and several differences in variable temperature magnetometry measurements were attributed to magnetic disorder induced by partial oxidation of the Co^{2+} ions in copper-deficient $Sr_2CoO_2Cu_{2-x}S_2$ [4].

$Sr_2CoO_2Ag_2Se_2$ and $Ba_2CoO_2Ag_2Se_2$ are both isostructural with $Sr_2CoO_2Cu_2S_2$, as shown by previous work [5,6]. Both these compounds were shown to be insulators using electrical transport measurements. Magnetic susceptibility measurements revealed broad maxima at 200–250 K, characteristic of antiferromagnetic ordering that is primarily two-dimensional in character [5,6]. This work extends the characterisation of these compounds by using powder neutron diffraction to characterise the magnetic ordering behaviour of these compounds at low temperatures, enabling comparison with the analogues containing copper sulfide layers.

* Corresponding author.
E-mail address: simon.clarke@chem.ox.ac.uk (S.J. Clarke).

https://doi.org/10.1016/j.jssc.2018.05.018
Received 20 March 2018; Received in revised form 9 May 2018; Accepted 13 May 2018
Available online 15 May 2018

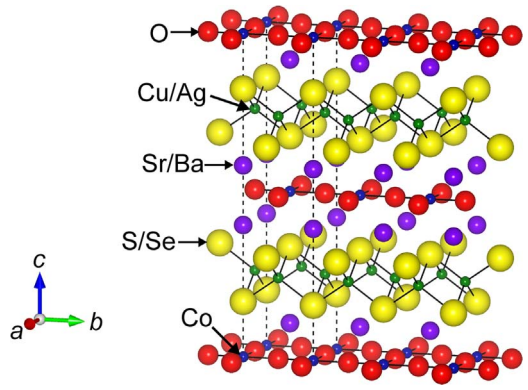

Fig. 1. The crystal structure of $A_2CoO_2M_2Ch_2$, where A = Sr, Ba; M = Cu, Ag and Ch = S, Se.

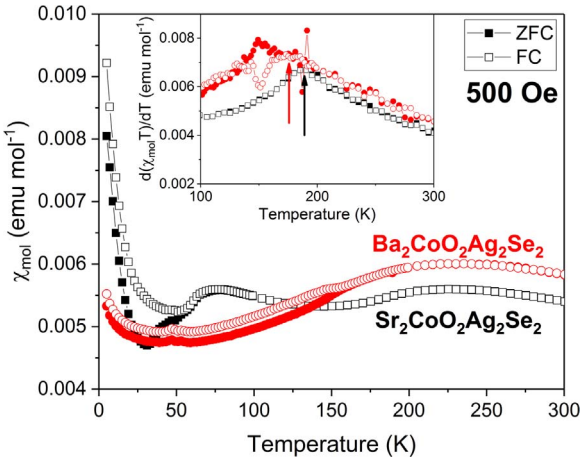

Fig. 2. The ZFC and FC magnetic susceptibility of $Sr_2CoO_2Ag_2Se_2$ and $Ba_2CoO_2Ag_2Se_2$. The inset shows the first derivative d(χT)/dT, with arrows corresponding to the regions that were identified as T_N.

2. Experimental

2.1. Synthesis

$A_2CoO_2Ag_2Se_2$ (A = Sr, Ba) samples were made by solid state sintering of a pressed pellet of Se (Alfa Aesar 99.999%), Co (Alfa Aesar Puratronic 99.998%), Ag (99.995% Sigma Aldrich) and BaO (99.99% Sigma Aldrich) or SrO respectively. Pure SrO (according to laboratory PXRD) was prepared from thermal decomposition of $SrCO_3$ (Alfa Aesar 99.995%) by heating it for 18 h at 850 °C and for a further 6 h at 1100 °C under dynamic vacuum. The reactants were ground thoroughly in an argon-filled glove box and pressed into one pellet, then loaded into an alumina crucible. Finally, the crucible was sealed in a dried silica tube under vacuum and heated in a furnace for 2 days at 835 °C ($Sr_2CoO_2Ag_2Se_2$) or 825 °C ($Ba_2CoO_2Ag_2Se_2$).

2.2. Diffraction measurements

Initial structural characterisation was carried out by powder X-ray diffraction (PXRD) using a PANalytical X'Pert pro instrument operating in Bragg-Brentano geometry with a Ge(111) monochromator to select CuKα$_1$ radiation. 3–4 g samples of $Sr_2CoO_2Ag_2Se_2$ and $Ba_2CoO_2Ag_2Se_2$ were measured using powder neutron diffraction (PND) at room temperature and 5 K in order to determine the magnetic structure of each compound. $Sr_2CoO_2Ag_2Se_2$ was measured using the constant-wavelength diffractometer D2B at the Institut Laue Langevin (ILL), Grenoble, France. 1.59 Å neutrons were selected by a Ge(115) crystal monochromator and detected using a multi-angle detector. $Ba_2CoO_2Ag_2Se_2$ was measured using the time-of-flight neutron diffractometer POLARIS at ISIS, Didcot, UK using data banks at 35, 90 and 145 degrees 2θ [7]. Rietveld refinement against both PND and PXRD data were conducted using the TOPAS Academic Version 5 software [8]. The magnetic structure was determined using ISODISTORT [9] in conjunction with TOPAS Academic.

2.3. Magnetometry measurements

Magnetometry measurements were performed on 20–80 mg portions of powder contained in gelatin capsules, using a Quantum Design MPMS-5 SQUID magnetometer. Measurements as functions of temperature in the range $5 \le T$ (K) ≤ 300 were carried out on warming in an applied magnetic field of 100 Oe after cooling in zero applied field (Zero-Field-Cooled (ZFC)) and subsequently after cooling in the measuring field (Field-Cooled (FC)).

3. Results and discussion

The samples prepared with compositions of $Sr_2CoO_2Ag_2Se_2$ and $Ba_2CoO_2Ag_2Se_2$ appeared to be phase pure by laboratory PXRD and adopted the same structure, with comparable lattice parameters to those reported previously [5,6]. This suggests that the compounds are stoichiometric, and this was supported by our PND measurements (see below). Magnetometry measurements, were consistent with those previously reported [5,6]. The magnetic susceptibilities of both $Sr_2CoO_2Ag_2Se_2$ and $Ba_2CoO_2Ag_2Se_2$, shown in Fig. 2, exhibited broad maxima in the region 200–250 K. These broad susceptibility features are commonly found in low-dimensional antiferromagnetic systems in which two-dimensional correlations resulting from strong intra-plane superexchange build and, on further cooling, long range three-dimensional magnetic ordering results from the effect of weaker inter-plane superexchange interactions [10–12]. The first derivative of the magnetic susceptibility (Fig. 2 inset) revealed maxima at 190 K and 180 K for $Sr_2CoO_2Ag_2Se_2$ and $Ba_2CoO_2Ag_2Se_2$. These maxima are assigned as the Néel temperatures (T_N) for long-range three-dimensional magnetic ordering, and this is consistent with the temperature where magnetic Bragg peaks appear in the isostructural $Ba_2CoO_2Cu_2S_2$ [4], and in measurements on several other two-dimensional systems [10–12].

Both compounds exhibit divergence of the ZFC and FC magnetic susceptibility curves at temperatures below the broad maxima, indicating history-dependent behaviour and possibly resulting from a minority disordered (i.e. spin-glass-like) component to the magnetism at low temperatures or due to a very slight spin canting. For $Ba_2CoO_2Ag_2Se_2$ bifurcation occurs at ~ 160 K, for $Sr_2CoO_2Ag_2Se_2$ it occurs at the lower temperature of ~ 60 K, below a second susceptibility maximum, of uncertain origin. Both Jin et al. [5] and Zhou et al. [6] note that this double maximum feature is also observed in La_2CoO_4, and in that case it arises from a spin-reorientation transition [13]. The variable temperature PND measurements of Smura et al. [4] did not show any evidence for any spin-reorientation transition in $Ba_2CoO_2Cu_2S_2$ which also shows a double maximum in the susceptibility, so we presume that the behaviour is unrelated to that of La_2CoO_4. Curie and Weiss constants could not be extracted from the data on $Sr_2CoO_2Ag_2Se_2$ and $Ba_2CoO_2Ag_2Se_2$ because the measurements were not made at temperatures much higher than those of the antiferromagnetic transitions. A small feature in the magnetic susceptibility of $Ba_2CoO_2Ag_2Se_2$ is also observed in the temperature range 45–50 K. This is not observed by Zhou et al. [6] so we ascribe it to a small amount of impurity below the level detectable by diffraction methods.

Refinement against the room temperature PND data confirmed the structural models previously found [5,6]. Previously we have shown that refinements against PND data from D2B and POLARIS are able to quantify non-stoichiometry that can occur in related compounds due to vacancies in the chalcogenide layer (i.e. Ag site vacancies in the present case) [4,14]. The refinements did not reveal any non-stoichiometry,

consistent with the high purity of the samples obtained in stoichiometric reactions. The Rietveld plots are shown in Fig. 3 and the refined parameters are shown in Table 1. Further databanks of the time-of-flight PND refinement of $Ba_2CoO_2Ag_2Se_2$ may be found in the supporting information.

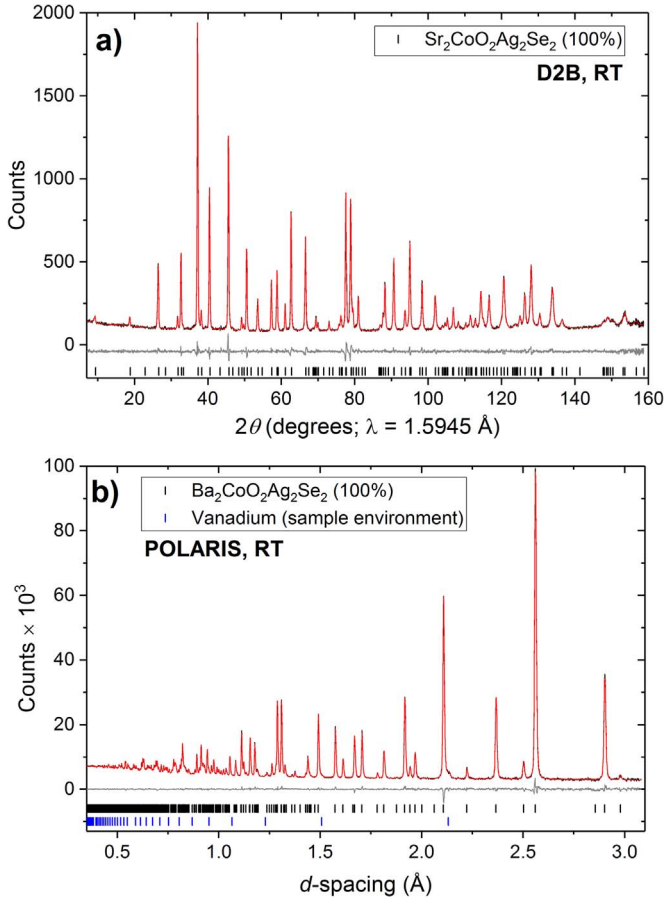

Fig. 3. Rietveld refinements against powder neutron diffraction data collected for a) $Sr_2CoO_2Ag_2Se_2$ using the fixed-wavelength diffractometer D2B (ILL) and b) $Ba_2CoO_2Ag_2Se_2$ using the time-of-flight diffractometer POLARIS (ISIS).

Table 1
Rietveld refinement results against powder neutron diffraction data for $Sr_2CoO_2Ag_2Se_2$ and $Ba_2CoO_2Ag_2Se_2$.

Compound	$Sr_2CoO_2Ag_2Se_2$	$Ba_2CoO_2Ag_2Se_2$
Radiation	Neutron, constant wavelength	Neutron, time-of-flight
Instrument	D2B, ILL	POLARIS, ISIS
Temperature	298(2)	
Space group	*I*4/*mmm*	
a (Å)	4.10210(6)	4.21471(8)
c (Å)	19.4265(3)	20.0193(5)
Volume (Å^3)	326.89(1)	355.62(2)
z(Sr/Ba)[a]	0.41682(7)	0.41233(4)
z(Se)[a]	0.15535(6)	0.16187(3)
U_{11}(Sr/Ba) (Å^2)	0.0036(5)	0.0012 (5)
U_{33}(Sr/Ba) (Å^2)	0.0094(8)	0.0043 (8)
U_{iso}(Co)[b] (Å^2)	0.004(1)[b]	0.0076(8)
U_{11}(O) (Å^2)	0.005(1)	0.0065(8)
U_{22}(O) (Å^2)	0.003(1)	0.014(1)
U_{33}(O) (Å^2)	0.010(1)	0.006(1)
U_{11}(Ag) (Å^2)	0.016(1)	0.0072(8)
U_{33}(Ag) (Å^2)	0.016(1)	0.017(1)
U_{11}(Se) (Å^2)	0.0055(5)	0.0077(4)
U_{33}(Se) (Å^2)	0.0072(7)	0.0067(5)
R_{wp} (%)	4.378	4.002

[a] Sr/Ba, 4*e*(0,0,*z*); Co, 2*a*(0,0,0); O, 4*c*(0,½,0); Ag, 4*d*(0,½,¼); Se, 4*e*(0,0,*z*).
[b] The Co atom was refined using an isotropic thermal displacement model.

PND data collected at 5 K revealed the presence of Bragg peaks that were not observed at room temperature. These Bragg peaks were found at long *d*-spacings and were indexed using a $\sqrt{2}a \times \sqrt{2}a \times c$ expansion

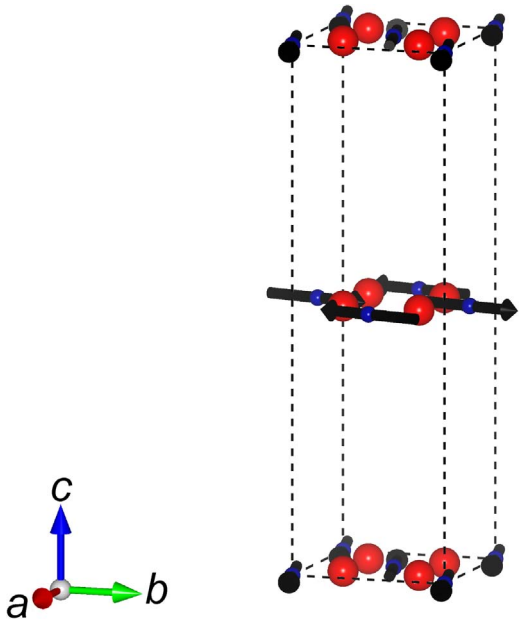

Fig. 4. The magnetic structure of $Sr_2CoO_2Ag_2Se_2$ and $Ba_2CoO_2Ag_2Se_2$, for clarity only the cobalt (small blue spheres) and oxide (large red spheres) ions are shown. (For interpretation of the references to color in this figure legend, the reader is referred to the web version of this article.)

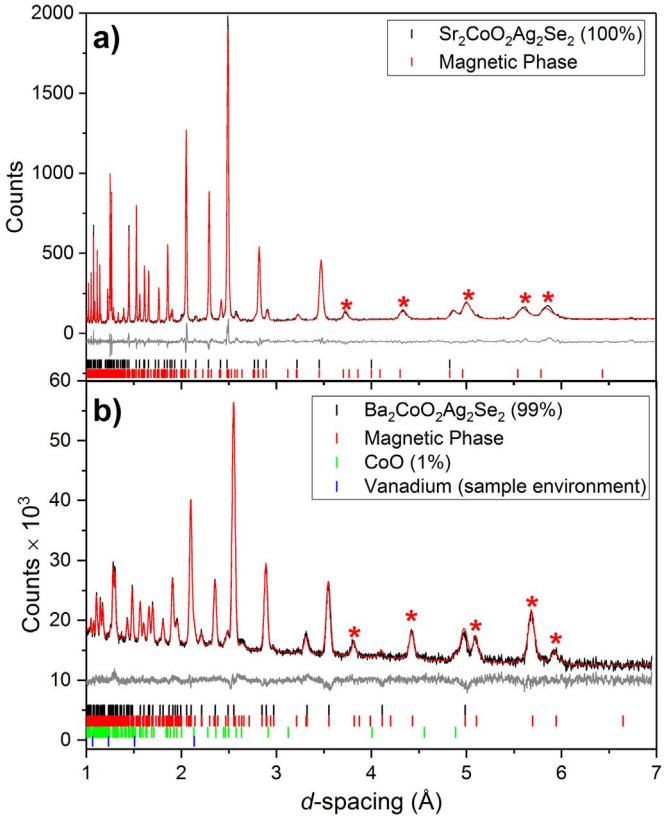

Fig. 5. Rietveld plots of a) $Sr_2CoO_2Ag_2Se_2$ and b) $Ba_2CoO_2Ag_2Se_2$ measured at 5 K using powder neutron diffraction. $Sr_2CoO_2Ag_2Se_2$ was measured using the constant-wavelength diffractometer D2B (ILL), while $Ba_2CoO_2Ag_2Se_2$ was measured on POLARIS (ISIS) (shown here is the A (35°) bank of the time-of-flight diffractometer). Both powder neutron diffraction patterns are shown plotted as functions of d-spacing for comparison.

Table 2
Refined magnetic moments of $Sr_2CoO_2Ag_2Se_2$ and $Ba_2CoO_2Ag_2Se_2$, measured at 5 K, using powder neutron diffraction. The magnetic structure was modelled using a non-collinear (tetragonal) model as discussed in the main text.

Compound	$Sr_2CoO_2Ag_2Se_2$	$Ba_2CoO_2Ag_2Se_2$
Temperature (K)	5	
Magnetic space group	P_C4_2/n (BNS scheme)	
μ_a (μ_B)	0.7(1)	0.80(3)
μ_b (μ_B)	3.7(1)	3.89(3)
μ_c (μ_B)	0	0
$\|\mu\|$ (μ_B)	3.7(1)	3.97(3)

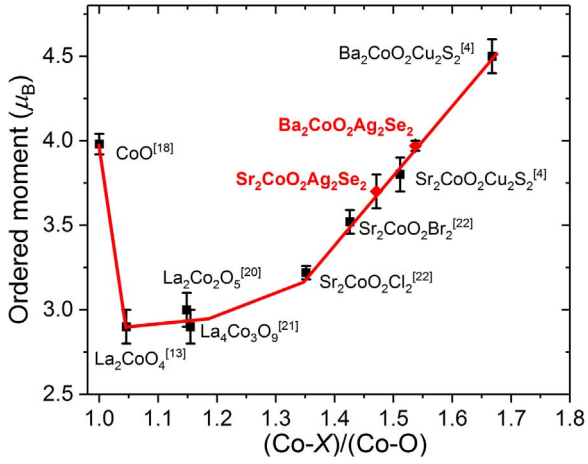

Fig. 6. Changing magnetic moment of Co^{2+} as a function of the coordination geometry from the literature (black) and from this work (red). Literature values are used for the bond lengths in the oxides [13,18,20,21], oxyhalides [22], and oxysulfides [4] with average values for the axial (×2) and equatorial (×4) Co–O bond lengths for systems with lower than D_{4h} symmetry at Co^{2+}. The line is a guide to the eye. (For interpretation of the references to color in this figure legend, the reader is referred to the web version of this article.)

of the nuclear unit cell, suggesting that they resulted from long-range antiferromagnetic ordering.

The intensity of the magnetic peaks was modelled using the activation of magnetic symmetry modes, initially in the magnetic space group $P1$ (1.1). A good fit to the data could not be achieved using any single magnetic symmetry mode; therefore combinations of modes were considered. It was found that three different modes could be activated which resulted in intensity at the positions of the magnetic peaks without resulting in magnetic intensity elsewhere. These modes were $mX2^+$(a), $mX3^+$(a) and $mX4^+$(a) and are shown in Fig. S5. The best fit to the data was obtained for both $Sr_2CoO_2Ag_2Se_2$ and $Ba_2CoO_2Ag_2Se_2$ when the $mX3^+$(a) and $mX4^+$(a) modes were refined together. The combination of these two magnetic modes resulted in nearest-neighbour antiferromagnetic interactions in the *ab*-plane, with no component in the *c*-axis, as shown in Fig. 4.

Once the magnetic symmetry modes had been identified, the P_C4_2/n magnetic space group (86.72 in the Belov, Neronova and Smirnova (BNS) scheme; a setting of P_p4_2/m' (84.7.719) in the Opechowski and Guccione (OG) scheme) [15] was found to be the highest-symmetry magnetic space group that could accommodate the distortion of both these magnetic modes. The results are shown in the Rietveld plot in Fig. 5 and Table 2. We note that in principle we cannot distinguish this model in which moments in adjacent planes are non-collinear from a model in which they are collinear [16] but the non-collinear model does enable retention of tetragonal symmetry.

The magnetic structures of $Sr_2CoO_2Ag_2Se_2$ and $Ba_2CoO_2Ag_2Se_2$ are similar to one another, the sole difference being a slightly larger magnitude of the ordered Co^{2+} moment in $Ba_2CoO_2Ag_2Se_2$. However, the magnitudes of the refined moments are within three standard deviations of one another.

It is known that high-spin d^7 Co^{2+} ions in an octahedral coordination carry an unquenched orbital contribution to the magnetic moment, resulting in ordered moments with a magnitude greater than the 3 μ_B expected if spin-only contributions are considered [17]. This is observed for CoO [18,19]. Reduction in the local Co symmetry from octahedral results in significant quenching of the orbital moment, but examination of a large number of oxide chalcogenide and oxide halide systems containing Co^{2+} revealed [4] that the orbital moment recovered as the distorted octahedral environment became increasingly distended, with the total ordered moment eventually exceeding that in CoO when the coordination environment approached square planar. This experimental observation was supported using a computational comparison of $Sr_2CoO_2Cu_2S_2$ and $Ba_2CoO_2Cu_2S_2$ [4]. Fig. 6 shows a plot of ordered moment as a function of the ratio (Co-*X*)/(Co-O) where *X* is the axial anion O, chalcogenide or halide. Because of the increased sizes of the Ag^+ cation and the Se^{2-} anion compared with the Cu^+ cation and S^{2-} anion, the (Co-*X*)/(Co-O) ratio is smaller in $Sr_2CoO_2Ag_2Se_2$ and $Ba_2CoO_2Ag_2Se_2$ than in their counterparts with copper sulfide layers, as shown in Table 3. The ordered magnetic moments of $Sr_2CoO_2Ag_2Se_2$ and $Ba_2CoO_2Ag_2Se_2$ are thus reduced in line with the trend, previously established by Smura et al. [4].

4. Conclusions

The magnetic structures of $Sr_2CoO_2Ag_2Se_2$ and $Ba_2CoO_2Ag_2Se_2$ have been deduced and refined from powder neutron diffraction data. The long-range antiferromagnetic ordering of the localised Co^{2+} moments is consistent with the expectation of antiferromagnetic superexchange between like moments mediated by 180° superexchange via intervening oxide ions. The two compounds are shown to conform to a relationship for related compounds in which the magnitude of the large unquenched orbital contribution to the magnetic moment in the ordered phase is governed by the degree of distortion of the CoO_4X_2 distended octahedral environment. Measurements on single crystals, including neutron spectroscopy, would be required to probe the subtleties evident in the susceptibility measurements in the magnetically ordered regime, and to determine the values of exchange constants.

Table 3
Comparison of the bond distances and angles of $Sr_2CoO_2Ag_2Se_2$ and $Ba_2CoO_2Ag_2Se_2$ with those of $Sr_2CoO_2Cu_2S_2$ and $Ba_2CoO_2Cu_2S_2$ (data obtained from Ref. [4]). All data was obtained from refinement against powder neutron diffraction data collected at room temperature.

Compound	$Sr_2CoO_2Cu_2S_2$ [4]	$Ba_2CoO_2Cu_2S_2$ [4]	$Sr_2CoO_2Ag_2Se_2$	$Ba_2CoO_2Ag_2Se_2$
Sr/Ba-O (Å)×4	2.5803(2)	2.7261(3)	2.6103(9)	2.7419(6)
Sr/Ba-*Ch* (Å) ×4	3.1491(3)	3.2675(5)	3.2218(8)	3.3300(5)
Co-O (Å)×4	1.99565(1)	2.03210(2)	2.05105(3)	2.10736(4)
Co-*Ch* (Å)×2	3.0327(5)	3.3721(9)	3.0169(12)	3.2397(5)
Co-O/Co-*Ch*	1.5197(3)	1.6594(4)	1.4709(6)	1.5373(2)
Cu/Ag-*Ch* (Å)×4	2.4356(3)	2.4395(5)	2.7553(8)	2.7490(3)
Ch-Cu/Ag-*Ch* (°)×4	109.19(1)	107.82(2)	116.48(2)	114.351(9)
Ch-Cu/Ag-*Ch* (°)×2	110.04(2)	112.82(4)	96.22(4)	100.100(17)

Acknowledgements

This work was supported by the UK EPSRC (Grant numbers EP/M020517/1 and EP/P018874/1). We thank the ISIS pulsed neutron and muon source and the Institut Laue Langevin for the award of neutron beam time. We thank the Diamond Light Source for studentship support for JNB. We are grateful to Dr. R I Smith for support on POLARIS and Dr E Suard for support on D2B.

Competing interests

The authors declare no competing interests.

Appendix A. Supporting information

Supplementary data associated with this article can be found in the online version at doi:10.1016/j.jssc.2018.05.018.

References

[1] W.J. Zhu, P.H. Hor, A.J. Jacobson, G. Crisci, T.A. Albright, S.H. Wang, T. Vogt, $A_2Cu_2CoO_2S_2$ (A = Sr, Ba), a novel example of a square-planar CoO_2 layer, J. Am. Chem. Soc. 119 (1997) 12398–12399.

[2] E. Brechtel, G. Cordier, H. Schaefer, Oxidpnictides – preparation and crystal structure of $A_2Mn_3B_2O_2$ with A = Sr, Ba and B = As, Sb, Bi, Z. Naturforsch. B: A J. Chem. Sci. 34B (1979) 777–780.

[3] S.J. Clarke, P. Adamson, S.J.C. Herkelrath, O.J. Rutt, D.R. Parker, M.J. Pitcher, C.F. Smura, Structures, physical properties, and chemistry of layered oxychalcogenides and oxypnictides, Inorg. Chem. 47 (2008) 8473–8486.

[4] C.F. Smura, D.R. Parker, M. Zbiri, M.R. Johnson, Z.A. Gál, S.J. Clarke, High-spin cobalt(II) ions in square planar coordination: structures and magnetism of the oxysulfides $Sr_2CoO_2Cu_2S_2$ and $Ba_2CoO_2Cu_2S_2$ and their solid solution, J. Am. Chem. Soc. 133 (2011) 2691–2705.

[5] S. Jin, X. Chen, J. Guo, M. Lei, J. Lin, J. Xi, W. Wang, W. Wang, $Sr_2Mn_3Sb_2O_2$ type oxyselenides: structures, magnetism, and electronic properties of $Sr_2AO_2M_2Se_2$ (A = Co, Mn; M = Cu, Ag), Inorg. Chem. 51 (2012) 10185–10192.

[6] T. Zhou, Y. Wang, S. Jin, D. Li, X. Lai, T. Ying, H. Zhang, S. Shen, W. Wang, X. Chen, Structures and physical properties of layered oxyselenides $Ba_2MO_2Ag_2Se_2$ (M = Co, Mn), Inorg. Chem. 53 (2014) 4154–4160.

[7] S. Hull, R.I. Smith, W.I.F. David, A.C. Hannon, J. Mayers, R. Cywinski, The polaris powder diffractometer at ISIS, Phys. B: Condens. Matter 180–181 (1992) 1000–1002.

[8] A.A. Coelho, TOPAS academic version 5, Coelho Software, Brisbane, Australia (2012).

[9] B.J. Campbell, H.T. Stokes, D.E. Tanner, D.M. Hatch, ISODISPLACE: a web-based tool for exploring structural distortions, J. Appl. Crystallogr. 39 (2006) 607–614 (ISODISTORT: ISOTROPY Software Suite, iso.byu.edu.).

[10] C.S. Knee, D.J. Price, M.R. Lees, M.T. Weller, Two- and three-dimensional magnetic order in the layered cobalt oxychloride Sr_2CoO_3Cl, Phys. Rev. B 68 (2003) 174407.

[11] J.B. He, D.M. Wang, H.L. Shi, H.X. Yang, J.Q. Li, G.F. Chen, Synthesis, structure and magnetic properties of the layered iron oxychalcogenide $Na_2Fe_2Se_2O$, Phys. Rev. B 84 (2011) 205212.

[12] N. Ni, E. Climent-Pascual, S. Jia, Q. Huang, R.J. Cava, Physical properties and magnetic structure of the layered oxyselenide $La_2O_3Mn_2Se_2$, Phys. Rev. B 82 (2010) 214419.

[13] K. Yamada, M. Matsuda, Y. Endoh, B. Keimer, R.J. Birgeneau, S. Onodera, J. Mizusaki, T. Matsuura, G. Shirane, Successive antiferromagnetic phase transitions in single-crystal La_2CoO_4, Phys. Rev. B 39 (1989) 2336–2343.

[14] M.J. Pitcher, C.F. Smura, S.J. Clarke, Stoichiometric CeOCuS – a well-behaved Ce(III) layered oxysulfide, Inorg. Chem. 48 (2009) 9054–9056.

[15] D.B. Litvin, Magnetic group tables: 1-, 2- and 3-dimensional magnetic subperiodic groups and magnetic space groups, Int. Union Crystallogr. (2013). http://dx.doi.org/10.1107/9780955360220001 (ISBN 978-0-9553602-2-0).

[16] G. Shirane, A note on the magnetic intensities of powder neutron diffraction, Acta Crystallogr. 12 (1959) 282–285.

[17] B.N. Figgis, M.A. Hitchman, Ligand Field Theory and its Applications, Wiley, New York, 2000.

[18] W. Jauch, M. Reehuis, H.J. Bleif, F. Kubanek, P. Pattison, Crystallographic symmetry and magnetic structure of CoO, Phys. Rev. B 64 (2001) 052102.

[19] W. Jauch, M. Reehuis, Electron density distribution in paramagnetic and antiferromagnetic CoO: a γ-ray diffraction study, Phys. Rev. B 65 (2002) 125111.

[20] O.H. Hansteen, H. Fjellvåg, B.C. Hauback, Crystal structure and magnetic properties of $La_2Co_2O_5$, J. Solid State Chem. 141 (1998) 411–417.

[21] O.H. Hansteen, H. Fjellvåg, B.C. Hauback, Crystal structure, thermal and magnetic properties of $La_4Co_3O_9$. Phase relations for $La_4Co_3O_{10-\delta}$ ($0.00 \le \delta \le 1.00$) at 673 K, J. Mater. Chem. 8 (1998) 2089–2093.

[22] C.S. Knee, M.T. Weller, Neutron diffraction study of crystal structure and antiferromagnetic order in $Sr_2CoO_2X_2$ (X = Cl, Br), Phys. Rev. B 70 (2004) 144406.